



Molecular dynamics simulation of homogeneous nucleation of melting in superheated sodium crystal

Tingting Ma ^{a,b,*}, Yang Li ^a, Kangning Sun ^a, Qinglin Cheng ^b, Sen Li ^{a,b}

^a Jiangsu Key Laboratory of Green Process Equipment, School of Petroleum and Natural Gas Engineering, School of Energy, Changzhou University, Changzhou 213164, PR China

^b School of Petroleum Engineering, Northeast Petroleum University, Daqing 163318, PR China



ARTICLE INFO

'Communicated by' Lijun Liu

Keywords:

Sodium
Molecular dynamics simulation
Equilibrium melting
Homogeneous nucleation

ABSTRACT

The melting process and nucleation behaviour of sodium (Na) crystals are crucial for the frozen start-up of high-temperature sodium heat pipes and the working performance of molten sodium batteries. Equilibrium melting and the homogeneous nucleation of melting in superheated Na crystal are studied by molecular dynamics simulation. The thermodynamic properties and nucleation of Na crystal during the heating process are investigated by the characterization of the density, radial distribution function (RDF), self-diffusion coefficient (D), nucleation rate (I_{hom}), etc. Firstly, the equilibrium melting of Na crystal is simulated and verified by the single-phase method. Results show that Na's equilibrium melting temperature, densities, and RDF simulated match well with experimental values, demonstrating that the EAM/FS potential is suitable for studying the melting processes of Na crystal. Secondly, the calculated D of liquid Na increases approximately linearly with rising temperature within 440 K~540 K and fits with experimental data well. The activation energy for the diffusion of Na obtained by linear fitting is $1.6406 \cdot 10^{20}$ J, which agrees well with the observed values. Finally, the homogeneous nucleation of melting in superheated Na crystal is analyzed. It is found that the I_{hom} of melting in superheated Na crystal rises exponentially with increasing temperature, which is consistent with the prediction in literature. The kinetic stability limit of superheated Na crystal is 468.3 K, and the relation between the I_{hom} of melting in superheated Na crystal and temperature is given. The physical properties and nucleation theory of Na crystal simulated during the melting can provide theoretical support for sodium's heat and mass transfer-related applications, such as sodium heat pipes and sodium batteries.

1. Introduction

Liquid alkali metals have the advantages of large latent heat of vaporization, low vapor pressure at high temperatures, and good thermal conductivity, which are used as heat transfer or energy storage medium, such as high-temperature heat pipes [1–3], nuclear reactors [4–5] and rechargeable batteries [6], etc. It is well known that alkali metals are usually solid at room temperature, so they must be melted into liquid before the elements work regularly. Accordingly, some scholars have taken high-temperature sodium heat pipes as the object to investigate their frozen start-up performance and thermal characteristics through experiments [2,7–9] and numerical simulation [4–5,10–11]. The results indicate that the normal start-up of the high-temperature sodium heat pipes in the early stage affects the working

performance. A few scholars have combined theories and experiments to study the nucleation behavior of sodium metal batteries. It is found that the nucleation behavior of metal Na anode melting is critically essential for the performance of rechargeable batteries [6]. These experiments and simulation studies about Na applications require the use of key parameters related to the melting and nucleation processes of Na crystals. However, for alkali metal Na, because of its high reactivity and handling with high temperatures, it is difficult to measure the physical properties and phase transition process by macroscopic experimental research [12], resulting in the lack of relevant parameters. So it is urgent to study them to provide a theoretical basis for their research. In recent years, with the development of computer technology and many-body potentials for describing metallic systems, the molecular dynamics (MD) method has been widely employed to simulate the melting process for titanium [13], iron [14], some alloys [15], as well as the evaporation

* Corresponding author at: Jiangsu Key Laboratory of Green Process Equipment, School of Petroleum and Natural Gas Engineering, School of Energy, Changzhou University, Changzhou 213164, PR China.

E-mail address: matt@cczu.edu.cn (T. Ma).

Nomenclature		<i>Greek symbols</i>	
<i>a</i>	lattice constant (Å)	ρ	electron density of an atom; density (g/cm ³)
<i>d</i>	the system's dimension	ϕ	pair potential interaction between atoms (eV)
<i>D</i>	self-diffusion coefficient (m ² /s)	ϵ	hydrostatic strain (%)
<i>D₀</i>	pre-exponential factor (m ² /s)	γ_{sl}	solid/liquid interfacial energy (J/cm ²)
ΔE	change of strain energy density (J/cm ³)	μ	shear modulus for crystalline solid (Gpa)
<i>F</i>	embedding function for atom	<i>Abbreviations</i>	
$g(r)$	radial distribution function	BCC	body-centered cubic
ΔG	Gibbs free energy change (J/cm ³)	EAM	embedded atom method
ΔG^*	critical work of nucleation (J)	FS	Finnis Sinclair
<i>h</i>	Planck constant (J·s)	LJ	Lennard Jones
I_{hom}	homogeneous nucleation rate (cm ⁻³ s ⁻¹)	MD	molecular dynamics
I_0	per-factor	MSD	mean square displacement
<i>k</i>	Boltzmann constant (J/K)	NPT	constant number, constant external pressure and constant temperature
<i>K</i>	bulk modulus for crystalline solid (Gpa)	NVT	constant number, constant volume and constant temperature
<i>N, n</i>	number of atoms in the system	RDF	radial distribution function
<i>Q</i>	activation energy for diffusion (J)	2NN	second nearest-neighbour
<i>r</i>	distance between atoms, radius of nucleation (Å)	MEAM	modified embedded atom method
r^*	the critical radius of nucleation (Å)	<i>Superscripts/Subscripts</i>	
<i>t</i>	simulation time (ps)	<i>c</i>	crystalline state
<i>T</i>	temperature (K)	<i>i</i>	atom <i>i</i>
T_0	experimental melting temperature (K)	<i>j</i>	atom <i>j</i>
T_m	equilibrium melting temperature (K)	<i>l</i>	liquid state
<i>V</i>	volume (Å ³)		
T_m^k	kinetic stability limit (K)		
ΔH_m	latent heat of fusion (J/cm ³)		
<i>U</i>	the total potential energy of the system (eV)		

and condensation characteristics of Na in high-temperature heat pipes [16–18], as it is unrestricted by the experimental conditions [14].

Melting is a phase transition from a long-range ordered crystalline state into a long-range disordered liquid form, usually divided into equilibrium and non-equilibrium melting processes. The heating temperature difference is minimal for the equilibrium melting. The temperature or pressure changes with time for the non-equilibrium melting process. Some scholars have applied the MD method to study the equilibrium melting process of perfect metal crystals, like copper [19–20], palladium [21], silver [22], etc., to determine their equilibrium melting temperature (T_m) and verify the rationality of the potential functions selected in simulation. Only a few scholars have studied the equilibrium melting processes of alkali metals through MD simulation. For example, Hasheminasab et al. [12] adopted the MD method with the potential of mean force and Lennard Jones (LJ) (5-4) to study the equilibrium melting of Na. The results show that the simulated radial distribution function (RDF) of liquid Na using the potential of mean force agrees well with the experimental values at 378 K. Still, the deviation gradually gets bigger at higher temperatures, both the mean force and LJ (5-4) potentials. Cui et al. [23] employed MD simulation with the second nearest-neighbour modified embedded atom method (2NN MEAM) potential to study the melting process of lithium (Li). It is shown that the simulated T_m of Li is 460 K, which is consistent with the experimental melting temperature (T_0). The RDFs of Li simulated also match well with the experimental values.

The melting processes of crystals have been experimentally proved to be nucleated at heterogeneous nucleation sites, such as free surfaces, grain boundaries, or defects [24]. When heterogeneous nucleation of melting at solid surfaces or interfaces is suppressed, e.g., utilizing proper coating with a high T_0 material [24], “removing” the covers of a crystal and ultrashort pulsed laser irradiation [25] methods, the solid phase persists in its metastable state above T_m , which is known as superheating of crystals. To understand the intrinsic melting mechanism and the superheating behaviour, the superheating of solids is usually analyzed

and estimated by kinetic considerations [24], just like the supercooling of liquids. Lu and Li [26] performed a kinetic analysis of homogeneous nucleation for melting in superheated aluminium crystals. It is found that the calculated homogeneous nucleation rate of melting in superheated aluminium crystal suddenly increases from essentially zero to a very high value around 1127 K, i.e., existing a critical temperature (T_m^k) at which a massive homogeneous nucleation catastrophe for melting occurs inside the superheated crystal lattice. Here, the T_m^k is known as the superheating temperature at which one nucleus is formed per second per cubic centimetre and is also called the kinetic stability limit for melting in a superheated crystal. According to the analysis, the T_m^k of Al is about 1.21 times the T_m . Meanwhile, the T_m^k for a series of transition metals, including iron, cobalt, nickel, etc., are also studied and given [24]. Summing up, Na crystal's melting process and homogeneous nucleation are rarely reported.

Thus, the equilibrium melting process of perfect Na crystal and the homogeneous nucleation of melting in superheated Na crystal are simulated by MD simulation in this paper. The physical properties of Na crystal melting and the homogeneous nucleation rate (I_{hom}) of melting in superheated Na crystal are obtained.

2. Simulation method

The EAM/FS potential is usually adopted to simulate the interaction between metal atoms, which can calculate the solid–liquid phase change and obtain the thermodynamic properties of metals [14]. The alkali metallic EAM/FS potential has been proposed for MD simulation. The total potential energy U of the system is denoted by the following equation [27]:

$$U = \sum_i F_i(\rho_i) + \frac{1}{2} \sum_{ij \neq i} \phi_{ij}(r_{ij}) \quad (1)$$

Where F_i is the embedding function for atom *i*, ρ_i is the electron density

of atom i embedded in the background, ϕ_{ij} is the pair potential interaction between atom i and j , and r_{ij} is the distance between atom i and atom j . In addition, for the details about Na's EAM/FS potential, please see the reference [27].

Fig. 1 shows the simulation flowchart model in this paper. Firstly, the original model of perfect Na crystal is shown in **Fig. 2**. The EAM/FS potential model between Na atoms proposed by Nichol [27] is employed. Among them, the size of the simulation system is $14 \times 14 \times 14 \cdot (a_{\text{Na}})^3$. The structure of Na cell is BCC (body-centered cubic) structure, and the lattice constant a_{Na} is 4.29 \AA . The total number of atoms is 5488 in this system. Then, we utilize the large-scale atomic/molecular massively parallel simulator (LAMMPS) open-source code to perform MD simulation of the equilibrium melting process of perfect Na crystal and homogeneous nucleation of melting in superheated Na crystal. The periodic boundary conditions are adopted in x , y , and z directions, and the Nose-Hoover method is applied to control the system's temperature and pressure. The system's initial pressure and temperature are set to 1 atm and 100 K, respectively. The verlet-velocity method is adopted to integrate the Newton equation, and the time step is set to be one fs.

Firstly, the equilibrium melting process of perfect Na crystal is simulated. The simulation system stabilizes at 100 K for 200 ps to reach thermodynamic equilibrium. Next, under the NPT (constant number, constant external pressure, and constant temperature) ensemble [28], the system is heated at a heating rate of 0.1 K/ps for every 5 K interval and then rebalanced for 100 ps until the system reaches 800 K. Outputting the density (ρ), volume, RDF and the atomic trajectory of Na at each time step, so as to determine the T_m of Na and verify the rationality of the selected EAM/FS potential model.

Secondly, the homogeneous nucleation for melting in superheated Na crystal is analyzed. The initial velocity distribution of Na atoms is given according to the Maxwell velocity distribution at 440 K, 460 K, 480 K, 500 K, 520 K, and 540 K, respectively. The system equilibrates at the NVT (constant number, constant volume, and constant temperature) ensemble [28] for 1.2 ns. The first 0.2 ns is employed to let the system reach thermodynamic equilibrium, and the rest of one ns is used to collect the data. Outputting the mean square displacement (MSD) of liquid Na at each time step to calculate the diffusion's activation energy (Q) value of liquid Na, and the homogeneous nucleation of melting in superheated Na crystal is analyzed to obtain the homogeneous nucleation rate (I_{hom}) and kinetic stability limit (T_m^k) of Na. Finally, the data simulated are analyzed and processed.

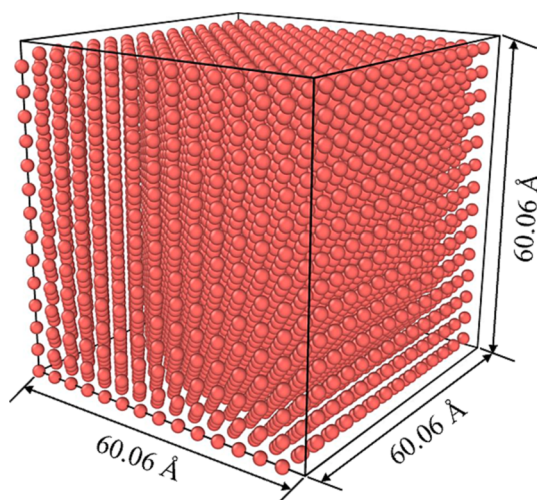


Fig. 2. The original model of the simulation system.

3. Results and discussion

3.1. Equilibrium melting of Na crystal and verification of the potential model

The equilibrium melting process of perfect Na crystal is simulated by the MD method. The calculated volume and density of Na at different temperatures during the melting process are shown in **Fig. 3**. It can be seen from **Fig. 3** that the volume and density of Na change sharply at the temperature range from 414 K to 419 K, corresponding to the solid-liquid phase transition process of Na, indicating that the T_m of Na simulated by the single-phase method is around 414 K, close to the experimental T_0 of 371 K [29], and the relative deviation is 11.6 %. In the simulation system, the Na atoms are solid below 414 K and liquid above 419 K. It can be found that the simulated T_m is slightly higher than the experimental T_0 , which is possibly attributed to the Na atoms in the model being perfect crystals with no interface and defects. In general, the Na used in the experiments is slightly impure, which leads to a higher overall energy and a lower T_0 [14]. Therefore, some deviations may exist between the simulated T_m and experimental T_0 .

Fig. 4 shows the simulated density of Na adopting EAM/FS potential compared with experimental values [30] at the temperature range from 300 K to 550 K. It can be seen from **Fig. 4** that the calculated density of Na decreases with increasing temperature, showing a trend of linear

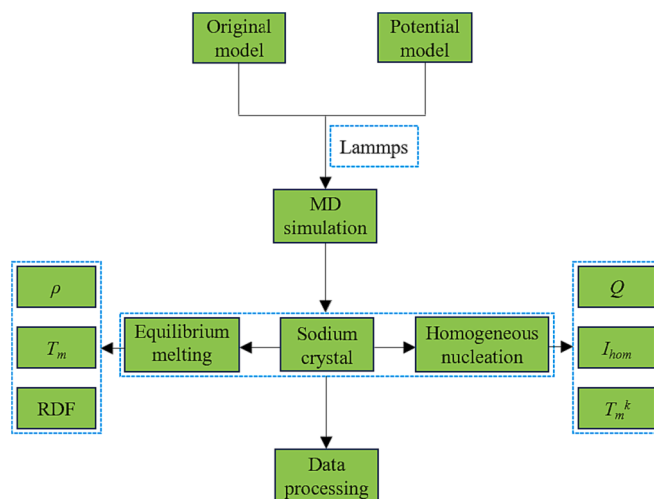


Fig. 1. The simulation flowchart model.

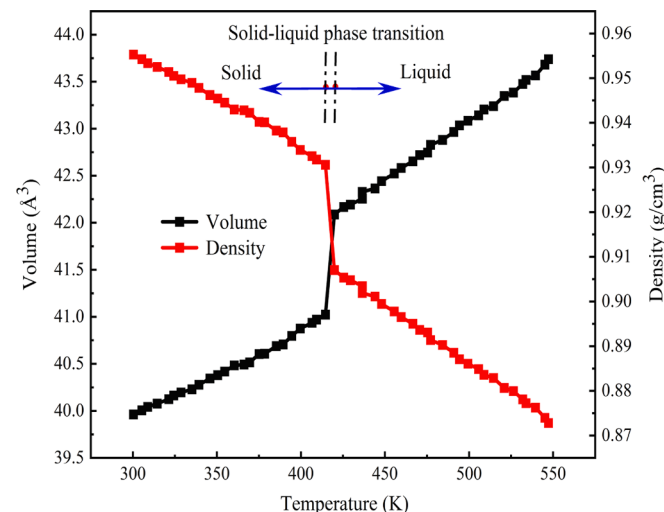


Fig. 3. Simulated volume and density of Na at different temperatures.

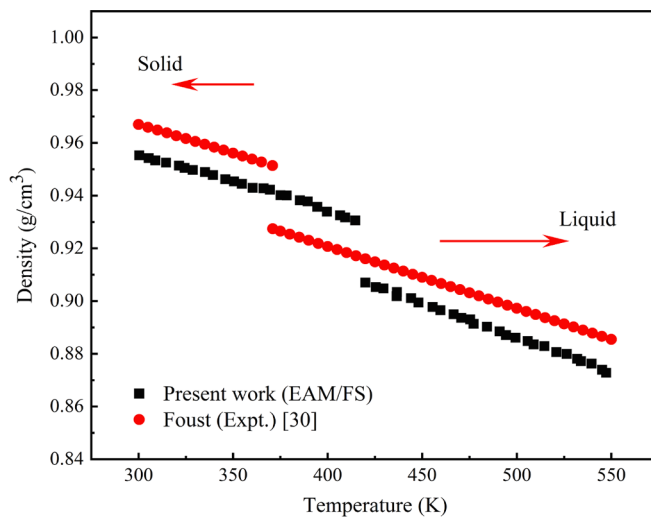


Fig. 4. A comparison of the calculated density of Na with experimental data.

change, and changes suddenly at 414 K, indicating that the Na crystal performs a solid–liquid phase transition at this temperature. However, the calculated density is lower than the experimental results within the temperature range of 300 K~550 K, and the maximum relative deviation between them is only 1.82 % at 547 K, which is possibly attributed to the slight difference in Na purity used in the simulation and experiment [14]. In conclusion, The T_m and ρ of Na calculated agree well with experimental data, indicating that the EAM/FS potential model is suitable for studying the equilibrium melting process of perfect Na crystal.

On this basis, it is necessary to investigate whether the EAM/FS potential model can describe the changes in the internal microstructure during Na melting from a microscopic perspective, and the RDF can achieve this purpose. RDF ($g(r)$) is a function adopted to characterize the disorder degree of the structural system, representing the probability of other atoms appeared in the space of radius (r) $\sim (r + dr)$ with one atom as the centre, which is denoted as the following [31]:

$$g(r) = \frac{2V}{N^2} \left\langle \sum_{i \neq j} \delta(r - r_{ij}) \right\rangle \quad (2)$$

Where V is the system's volume, N represents the number of atoms in the system, and r_{ij} is the distance between atom i and atom j , for the ordered lattice structure, the peaks of $g(r)$ occur at different neighbouring positions, the position and related magnitude of which is determined by the crystalline structure itself. Increasing the temperature can cause peaks to weaken or even disappear.

The calculated RDFs of Na at 223 K, 378 K, 573 K, and 723 K by adopting EAM/FS potential are compared with experimental values [32] and simulation results of other potentials [12] in Fig. 5(a)~(d), and the corresponding microstructures of Na are also given respectively. At 223 K and 378 K, it can be seen from Fig. 5(a)~(b) that the peaks of the $g(r)$ curve are high and narrow. Especially at 378 K, there is a clear “step” at 6.13 Å. The little and discrete peak exists at the same position before 378 K, as shown in Fig. 5(a), and it gradually decreases and forms with increasing temperature. Observing the corresponding microstructures of Na in the simulation system, it is found that the Na atoms are still vibrating near the equilibrium position and in a non-connected state, indicating that the Na is still in a solid state at 223 K and 378 K.

When the temperature is from 378 K to 573 K, from Fig. 5(c), it can be seen that the peaks of $g(r)$ simulated by EAM/FS potential become shorter and broader. The relative magnitude of the prominent peak of $g(r)$ decreases from 2.7 to 2.11, the “steps” on the curve disappear and integrate into the second peak, and the third peak disappears. Viewing the corresponding microstructures of Na in the system, it can be found

that the distribution of Na atoms is highly chaotic and in a completely disordered state [33], demonstrating that the Na is in liquid form at 573 K. We can also see from Fig. 5(c)~(d) that the $g(r)$ of liquid Na simulated employing EAM/FS potential at 573 K and 723 K perfectly agree with the experimental RDF. Compared with the simulation results of the mean force and LJ (5-4) potential in literature [12], the $g(r)$ curve of liquid Na calculated by EAM/FS potential is in better agreement with experimental data. Therefore, it is demonstrated that the employed EAM/FS potential is suitable to simulate the melting process of perfect Na crystal.

3.2. Homogeneous nucleation of melting in superheated Na crystal

Based on the equilibrium melting of Na investigated above, perform the kinetic analysis of homogeneous nucleation for melting in superheated Na crystal and calculate the I_{hom} for melting in superheated Na crystal. Since the Q value must be used, it is necessary to first calculate the Q of Na within a specific temperature range. Then, the kinetic analysis of homogeneous nucleation for melting in superheated Na crystal is carried out to calculate its I_{hom} .

3.2.1. Calculation of activation energy for the diffusion of Na

The calculation process of Q for Na in a specific temperature range is as follows: firstly, the MD simulation is applied to obtain the MSD with time within a particular temperature range. Then, the D (self-diffusion coefficient) of liquid Na at different temperatures is calculated by Einsteinian relation based on MSD. Finally, the Arrhenius equation based on D linearly fits the Q of Na within a specific temperature range.

MSD is the mean square of the particle displacement and is defined as the following [33]:

$$\text{MSD} = \frac{1}{N} \sum_{i=1}^N [r_i(t) - r_i(0)]^2 \quad (3)$$

In which N denotes the number of atoms in the system, r_i is the position of atom i .

Generally, the MSD oscillates around a specific value for the ordered crystalline structure, and for the disordered liquid form, the MSD increases linearly with the simulation time. Fig. 6 displays the MD results of MSD for liquid Na from 440 K to 540 K, based on EAM/FS potential. We can see that the MSD of liquid Na increases linearly with the increase of simulation time at different temperatures, and the slope of the curve increases with increasing temperature. Due to the growing distance between atoms, relative motion amplitude interaction between bound atoms weakens with increasing temperature [34].

The change of MSD with time characterizes the diffusion behavior of liquid metals, and the following Einsteinian relation exists with D [33]:

$$\lim_{t \rightarrow \infty} \text{MSD} = c + 2dDt \quad (4)$$

Where D is the self-diffusion coefficient, t represents the simulation time, c is constant, and d denotes the system's dimension, equal to 3.

According to Eq. (4), the slope of the curves in Fig. 6 can be applied to calculate D . The calculated D of liquid Na at different temperatures is shown in Fig. 7. The reported experimental values [35–36] and simulation results by other potentials [12,37–38] are also illustrated in Fig. 7. It indicates that the D of liquid Na increases approximately linearly with the increase of temperature, which is possibly related to the accelerating collision frequency between atoms with increasing temperature.

Moreover, it can be found that the D of liquid Na within 440 K~540 K simulated applying EAM/FS potential perfectly fits with the experimental D , which is measured by Ozelton et al. [35] employing the capillary filling technique under constant volume and constant pressure conditions. The maximum relative deviation from the experimental D by Meyer et al. [36] adopting the capillary reservoir technique is only 9.13 % at 480 K. There is a significant deviation from the D of liquid Na calculated by other potentials, especially the potential of mean force and

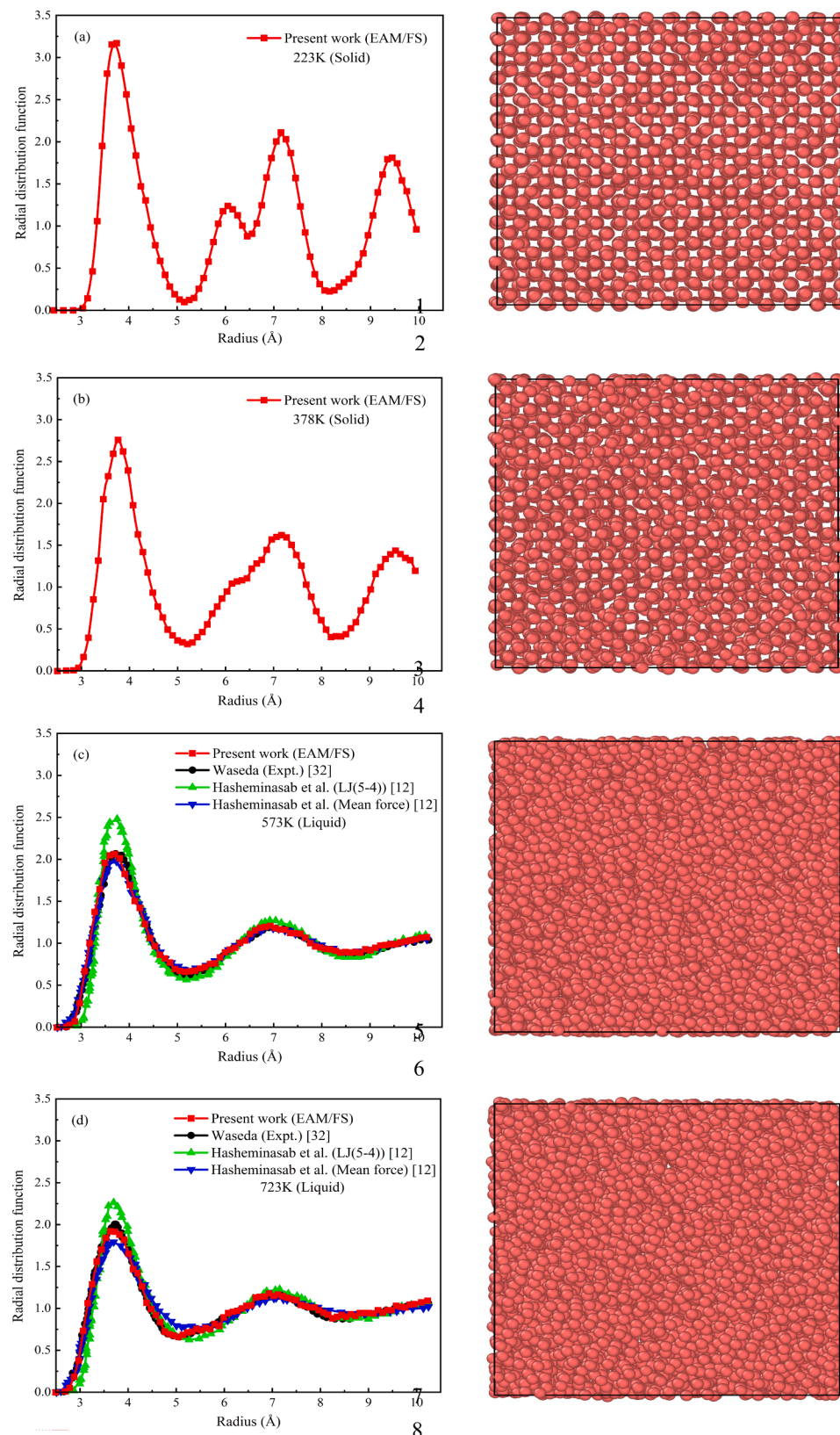


Fig. 5. Simulated RDFs of Na compared with experimental data and calculation results of other potentials, and corresponding microscopic structures of Na at different temperatures.

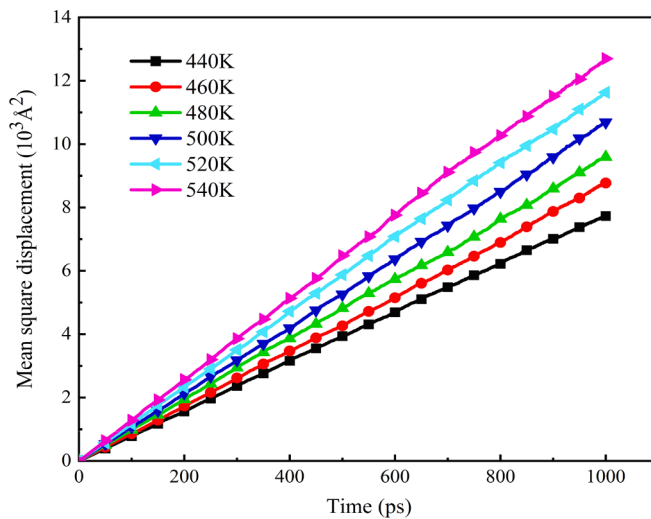


Fig. 6. Simulated MSD of liquid Na at different temperatures.

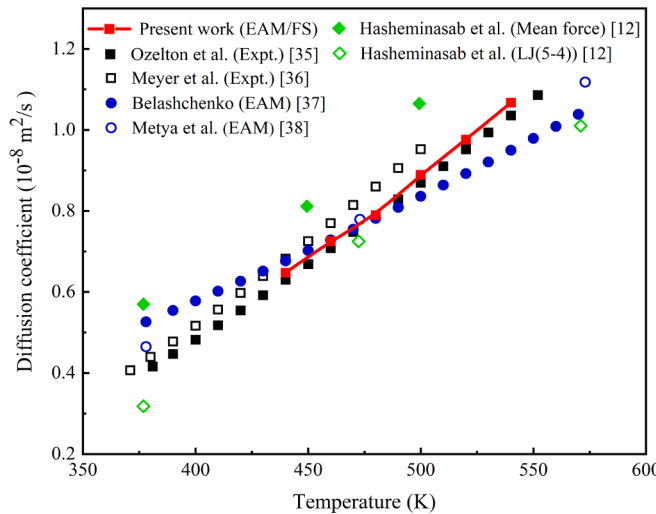


Fig. 7. Comparison of the simulated D of liquid Na with experimental data, and other potential simulations.

LJ (5-4) potential applied by Hasheminasab et al. [12], demonstrating that the different potentials lead to different simulation results. However, the general trend of the D of liquid Na with the temperature change consistently coincides. Accordingly, the simulated results show that the applied EAM/FS potential can also accurately calculate the D of liquid Na.

According to the transition state theory, the relationship between the D of a group of atoms in the simulation system and T can be expressed by the following Arrhenius equation that contains two constants, a pre-exponential factor, D_0 , and the activation energy for diffusion, Q [30]:

$$D = D_0 \exp\left(-\frac{Q}{kT}\right) \quad (5)$$

Where k is the Boltzmann constant, equal to $1.38 \cdot 10^{-23}$ J/K, and T is the temperature of Na. The above Arrhenius equation also can be written in the form as follows:

$$\ln D = \ln D_0 - \frac{Q}{kT} \quad (6)$$

Take $1/(kT)$ as the independent variable and $\ln D$ as the dependent variable, the Arrhenius figure for D of Na is plotted in Fig. 8. The D_0 of

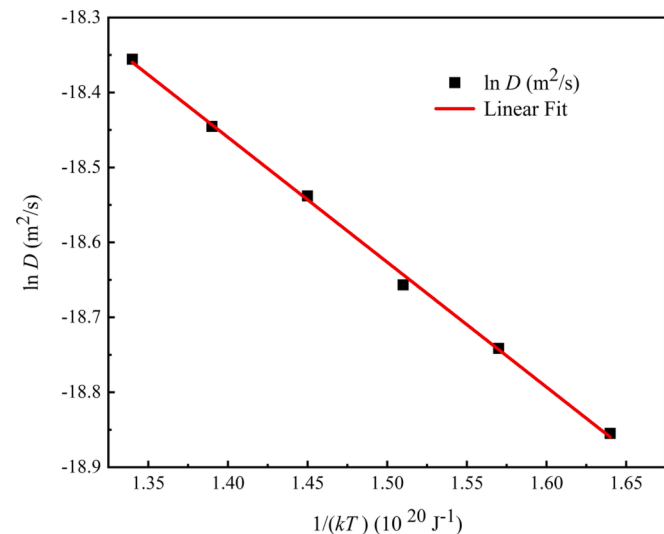


Fig. 8. The relation between $\ln D$ and $1/(kT)$ in the form of the Arrhenius equation of Na.

Na is fitted as $0.9585 \cdot 10^{-7}$ m²/s, and the Q is $1.6406 \cdot 10^{-20}$ J. Substitute the D_0 and Q into formula (6) to obtain the relation between D and T in the form of the Arrhenius equation of Na:

$$\ln D = \ln(0.9585 \cdot 10^{-7}) - \left(\frac{1.6406 \cdot 10^{-20}}{kT}\right) \quad (440 \text{ K} \leq T \leq 540 \text{ K}) \quad (7)$$

Only a few experimental results are reported about the D_0 and Q of Na. Table 1 lists the D_0 , Q , and corresponding expression as the Arrhenius equation of Na based on EAM/FS potential and experiments [35–36]. As shown in Table 1, the D_0 and Q of Na fitted by the Arrhenius formula agree well with the experimental values. The maximum relative deviation of Q compared with the experimental result in the literature [36] is about 3.62 %.

Through the MD simulation of the equilibrium melting of Na crystal and the fitting calculation of Q for Na, Na's T_m and Q values are 414 K and $1.6406 \cdot 10^{-20}$ J, respectively. Moreover, it can be demonstrated from Fig. 3 that the solid and liquid volumes V_c and V_l of Na at T_m are 41.02 Å^3 and 42.09 Å^3 , respectively.

3.2.2. Homogeneous nucleation rate of melting in superheated Na crystal

When the crystal is heated above its T_m , the Gibbs free energy difference between the solid and liquid phases drives the force for melting. The heterogeneous nucleation of melting can be restricted at defects, free surfaces, grain boundaries, or dislocations because of a suitable coating or heating internally. Only homogeneous nucleation of melting occurs inside the bulk crystal. A liquid spherical nucleus is formed inside a perfect crystalline lattice, and the Gibbs free energy change can be expressed as [26]:

$$\Delta G(T) = \frac{4}{3} \pi r^3 (\Delta G_v + \Delta E) + 4\pi r^2 \gamma_{sl} \quad (8)$$

Where r is the radius of nucleation, γ_{sl} denotes the solid/liquid interfacial energy, equal to $3.1 \cdot 10^{-6}$ J/cm² for Na [24], ΔG_v can be approximated by $\Delta H_m (T_m - T)/T_m$ (here ΔH_m represents the latent heat of fusion, which is 121.427 J/cm^3 for Na [39]), ΔE is the change of strain energy density per volume caused by the volume change during melting. It can be denoted as [26]:

$$\Delta E = \frac{18\mu K \varepsilon^3}{4\mu + 3K} \quad (9)$$

Where μ and K are the shear and bulk modulus for the crystalline solid, and their values are 3.3 Gpa and 6.3 Gpa for Na, respectively [29]. ε is

Table 1

D_0 , Q , and the corresponding formula in the form of Arrhenius equation of Na.

Literature	$D_0 (10^{-7} \text{ m}^2/\text{s})$	$Q (10^{-20} \text{ J})$	Corresponding expression	Temperature (K)
Present work (EAM/FS)	0.9585	1.6406	$\ln D = \ln(0.9585 \cdot 10^{-7}) - \left(\frac{1.6406 \cdot 10^{-20}}{kT} \right)$	$440 \text{ K} \leq T \leq 540 \text{ K}$
Ozelton et al. (Expt.) [35]	0.92	1.6279	$\ln D = \ln(0.92 \cdot 10^{-7}) - \left(\frac{1.6279 \cdot 10^{-20}}{kT} \right)$	$381 \text{ K} \leq T \leq 552 \text{ K}$
Meyer et al. (Expt.) [36]	1.10	1.7022	$\ln D = \ln(1.10 \cdot 10^{-7}) - \left(\frac{1.7022 \cdot 10^{-20}}{kT} \right)$	$371 \text{ K} \leq T \leq 499.5 \text{ K}$

the hydrostatic strain connected with the fractional volume change ($\Delta V/V_c$) upon melting, where ΔV is $(V_l - V_c)$.

Similar to the classical homogeneous nucleation theory for solidification [26], the critical radius of nucleation is obtained by calculating the extreme value of Eq. (8):

$$r^*(T) = \frac{-2\gamma_{sl}}{\Delta G_v + \Delta E} \quad (10)$$

The corresponding energy is a critical work of nucleation:

$$\Delta G^*(T) = \frac{16\pi\gamma_{sl}^3}{3(\Delta G_v + \Delta E)^2} \quad (11)$$

According to Mei and Lu [24,26], the I_{hom} of liquid can be calculated via

$$I_{hom} = I_0 \exp\left(-\frac{\Delta G^*(T)}{kT}\right) \exp\left(-\frac{Q}{kT}\right) \quad (12)$$

Where Q is the activation energy for atomic diffusion, I_0 is a per-factor associated with atomic vibration frequency and the surface area of the crystal nuclei, approximated by (nkT/h) (where n is the number of atoms in a unit volume, h is Planck constant, equal to $6.63 \cdot 10^{-34} \text{ J} \cdot \text{s}$).

It can be seen from Eq. (10) and Eq. (11) that the r^* and ΔG^* of homogeneous melting in superheated crystals are functions of temperature. Fig. 9 shows the calculated r^* and ΔG^* as a function of the temperature of homogeneous melting in superheated Na crystal. It is revealed that the r^* and ΔG^* decrease with increasing temperature, indicating that the energy barrier required to overcome homogeneous nucleation melting in superheated Na crystal is reduced, and it is easier to nucleate.

Take T as the independent variable and $\ln(I_{hom})$ as the dependent variable, the $\ln(I_{hom})$ of homogeneous melting in superheated Na crystal and its nonlinear fit with temperature are presented in Fig. 10. In Fig. 10, the I_{hom} of homogeneous melting in superheated Na crystal increases exponentially with the increase of temperature. It is consistent with the

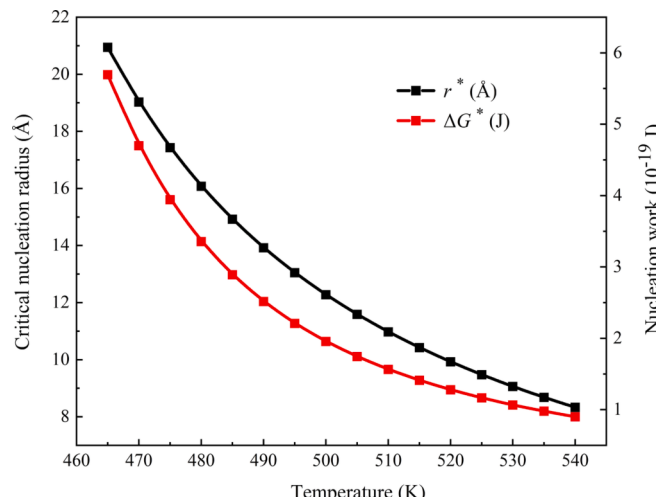


Fig. 9. r^* and ΔG^* of homogeneous melting in superheated Na crystal.

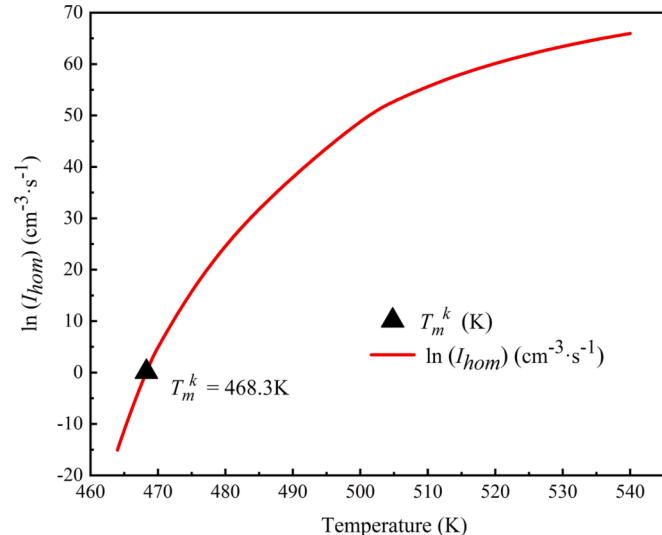


Fig. 10. The calculated and fitted $\ln(I_{hom})$ of homogeneous melting in superheated Na crystal with temperature.

expectation in the literature [26]. On the one hand, it can be demonstrated from Eq. (12) that the I_0 and the diffusion coefficient terms $\exp[-Q/(kT)]$ increase with rising temperature. On the other hand, the ΔG^* decreases with the temperature increase in Fig. 9, rising by driving force term $\exp[-\Delta G^*(T)/(kT)]$ with increasing temperature. The fitted calculation formula between the I_{hom} of homogeneous melting in superheated Na crystal and T is as follows:

$$\ln(I_{hom}) = -68.1830 + 30.9748 \ln(T - 458.9263) \quad (464 \text{ K} \leq T \leq 540 \text{ K}) \quad (13)$$

There is a critical temperature (T_m^k) of 468.3 K (about 1.13 times the T_m) in Fig. 10, at which the $\ln(I_{hom})$ for the superheated Na crystal is equal to zero, corresponding to one nucleus is formed per second per cubic centimetre under homogeneous nucleation of melting in superheated Na. From a kinetic point of view, the T_m^k is considered a kinetic stability limit for the superheated crystal, at which a massive homogeneous nucleation catastrophe for melting occurs inside the superheated crystal lattice [26].

In conclusion, the simulated physical properties of Na such as T_m , ρ , D , etc., and the formed homogeneous nucleation theory of melting in superheated Na crystals like the Q , I_{hom} , T_m^k , and so on can provide the essential physical parameters and solid–liquid phase transition laws for studying the related applications of Na, for example, analyzing the melting process of working medium in sodium heat pipes during frozen start-up, and the nucleation of metal Na anode melting in molten sodium batteries.

4. Conclusion

The equilibrium melting process of perfect Na crystal and the homogeneous nucleation of melting in superheated Na crystal are simu-

lated by the molecular dynamics method with EAM/FS many-body potential in this paper. Thermodynamic properties and nucleation of Na crystal during the heating process are investigated by the characterization of the ρ , D , Q , I_{hom} , etc. The main conclusions are as follows:

- (1) The Na's equilibrium melting temperature simulated employing the single-phase method is 414 K, and the relative deviation from the experimental value of 371 K is around 11.6 %. The calculated density and radial distribution function with temperature agree well with experimental data, indicating that the EAM/FS potential is suitable to simulate the melting process of Na crystal.
- (2) The simulated self-diffusion coefficient of liquid Na increases approximately linearly with increasing temperature within 440 K \sim 540 K, perfectly fitting with the experimental data. The activation energy for the diffusion of Na obtained by linear fitting is $1.6406 \cdot 10^{-20}$ J, which matches well with experimental values, and the maximum relative deviation is about 3.62 %. The relation between the self-diffusion coefficient of liquid Na and temperature can be described by the formula in the form of the Arrhenius equation:

$$\ln D = \ln(0.9585 \cdot 10^{-7}) - \left(\frac{1.6406 \cdot 10^{-20}}{kT} \right) \quad (440 \text{ K} \leq T \leq 540 \text{ K})$$

- (3) The calculated nucleation rate of homogeneous melting in superheated Na crystal rises exponentially with increasing temperature, which is consistent with the prediction in the literature. The kinetic stability limit calculated for superheated Na crystal is 468.3 K, about 1.13 times the equilibrium melting temperature. The relation between the nucleation rate of homogeneous melting in superheated Na crystal and the temperature obtained by nonlinear fitting can be described by the formula:

$$\ln(I_{hom}) = -68.1830 + 30.9748 \ln(T - 458.9263) \quad (464 \text{ K} \leq T \leq 540 \text{ K})$$

The physical properties and nucleation theory of Na crystal of homogeneous melting can provide a theoretical basis for avoiding failure start-up and achieving regular operation of the sodium heat pipes and helpful clues for the performance of sodium batteries and avoiding overheating.

CRediT authorship contribution statement

Ma Tingting: Methodology, Project administration, Funding acquisition, Writing – review & editing. **Li Yang:** Investigation, Software, Validation, Writing – original draft. **Sun Kangning:** Data curation, Formal analysis, Resources, Software. **Cheng Qinglin:** Conceptualization, Supervision. **Li Sen:** Project administration, Funding acquisition, Supervision.

Declaration of Competing Interest

The authors declare that they have no known competing financial interests or personal relationships that could have appeared to influence the work reported in this paper.

Data availability

Data will be made available on request.

Acknowledgements

We gratefully acknowledge the financial support from the special fund for Heilongjiang Provincial Postdoctoral Science Foundation [No. LBH-Z20118 and No. LBH-Z21125], and Scientific Research Foundation of Jiangsu Provincial Education Department [No. 21KJB470001].

References

- [1] Y. Ma, H. Yu, S. Huang, Y. Zhang, Y.u. Liu, C. Wang, R. Zhong, X. Chai, C. Zhu, X. Wang, Effect of inclination angle on the startup of a frozen sodium heat pipe, *Appl. Therm. Eng.* 201 (2022) 117625, <https://doi.org/10.1016/j.apithermaleng.2021.11>.
- [2] T.T. Ma, C.J. Zhu, Y. Li, et al., Experimental study on start-up performance of sodium heat pipe with metal-foam wick at different heating temperature [J], *Chin. J. Vacuum Sci. Technol.* 43 (08) (2023) 674–680, <https://doi.org/10.13922/j.cnki.cjvst.20230101>.
- [3] X. Wang, T. Ma, Y. Zhu, H. Chen, J. Zeng, Experimental investigation on startup and thermal performance of a high temperature special-shaped heat pipe coupling the flat plate heat pipe and cylindrical heat pipes [J], *Appl. Therm. Eng.* 77 (2016) 1–9, <https://doi.org/10.1016/j.expthermflusci.2016.03.013>.
- [4] Z. Zhang, X. Chai, C. Wang, H. Sun, D. Zhang, W. Tian, S. Qiu, G.H. Su, Numerical investigation on startup characteristics of high temperature heat pipe for nuclear reactor [J], *Nucl. Eng. Des.* 378 (2021) 111180.
- [5] Y. Yuan, J.L. Guo, J.Q. Shan, et al., Startup characteristics of heat pipe cooled space reactor. [J], *Atom. Energy Sci. Technol.* 50 (06) (2016) 1054–1059, <https://doi.org/10.7538/yzk.2016.50.06.1054>.
- [6] H. Wang, E. Matios, J. Luo, W. Li, Combining theories and experiments to understand the sodium nucleation behavior towards safe sodium metal batteries [J], *Chem. Soc. Rev.* 49 (12) (2020) 3783–3805, <https://doi.org/10.1039/docrs00033g>.
- [7] W.F. Teng, X.Y. Wang, Y.Z. Zhu, Experimental investigations on start-up and thermal performance of sodium heat pipe under swing conditions [J], *Int. J. Heat Mass Transf.* 152 (2020), 119505, <https://doi.org/10.1016/j.ijheatmasstransfer.2020.119505>.
- [8] C. Wang, D. Zhang, S. Qiu, W. Tian, Y. Wu, G. Su, Study on the characteristics of the sodium heat pipe in passive residual heat removal system of molten salt reactor [J], *Nucl. Eng. Des.* 265 (2013) 691–700, <https://doi.org/10.1016/j.nucengdes.2013.09.023>.
- [9] T. Ma, Y. Zhu, H. Chen, X. Wang, J. Zeng, B. Lu, Frozen start-up performance of a high temperature special shaped heat pipe suitable for solar thermochemical reactors [J], *Appl. Therm. Eng.* 109 (2016) 591–599, <https://doi.org/10.1016/j.apithermaleng.2016.08.091>.
- [10] X. Wang, Y. Shi, T. Liu, S. Wang, K. Wang, H. Chen, Y. Wang, Y. Zhu, CFD modeling of liquid-metal heat pipe and hydrogen inactivation simulation [J], *Int. J. Heat Mass Transf.* 199 (2022) 123490.
- [11] Z.Q. Zhang, C.L. Wang, H. Sun, et al., Analysis of startup characteristics for alkali metal high temperature heat pipe. [J], *Atom. Energy Sci. Technol.* 55 (06) (2021) 1015–1023, <https://doi.org/10.7538/yzk-2020.youxian.0464>.
- [12] F. Hasheminasab, N. Mehdipour, Molecular dynamics simulation of fluid sodium [J], *Fluid Phase Equilib.* 427 (2016) 161–165, <https://doi.org/10.1016/j.fluid.2016.07.008>.
- [13] J. Jiang, X. Zhang, F. Ma, S. Dong, W. Yang, M. Wu, Molecular dynamics simulation of the crystal structure evolution of titanium under different Tdamp values and heating/cooling rates [J], *Chem. Phys. Lett.* 763 (2021) 138187.
- [14] H.-J. Yan, J.-C. Zhuang, P. Zhou, Q. Li, C.Q. Zhou, P. Fu, Molecular dynamics simulation of thermal physical properties of molten iron [J], *Int. J. Heat Mass Transf.* 109 (2017) 755–760, <https://doi.org/10.1016/j.ijheatmasstransfer.2017.02.027>.
- [15] D.E. Farache, J.C. Verduzco, Z.D. McClure, S. Desai, A. Strachan, Active learning and molecular dynamics simulations to find high melting temperature alloys, *Comput. Mater. Sci.* 209 (2022) 111386, <https://doi.org/10.48550/arXiv.2110.08136>.
- [16] Z. Wang, R. Han, K. Guo, C. Wang, D. Zhang, W. Tian, S. Qiu, G. Su, Molecular dynamics simulation of the evaporation of liquid sodium film in the presence of non-condensable gas, *Ann. Nucl. Energy* 170 (2022) 109005, <https://doi.org/10.1016/j.anucene.2022.109005>.
- [17] Z.T. Wang, K.L. Guo, C.L. Wang, et al., Molecular dynamics study of characters of evaporation and condensation of sodium inside high temperature pipe [J], *Atom. Energy Sci. Technol.* 56 (07) (2022) 1267–1275, <https://doi.org/10.7538/yzk.2021.youxian.0350>.
- [18] Z.T. Wang, K.L. Guo, C.L. Wang, et al., Molecular dynamics study of mass accommodation coefficient of liquid-gas interface inside sodium heat pipe [J], *Atom. Energy Sci. Technol.* 56 (06) (2022), <https://doi.org/10.7538/yzk.2021.youxian.0905>.
- [19] H.L. Wang, X.X. Wang, H.Y. Liang, Molecular dynamics simulation and analysis of bulk and surface melting processes for metal Cu [J], *Acta Metall. Sin.* 41 (06) (2005) 568–572, <https://doi.org/10.3321/j.issn:0412-1961.2005.06.002>.
- [20] T. Zhang, X.R. Zhang, L. Guan, et al., The simulation of metal Cu in the melting and solidification process [J], *Acta Metall. Sin.* 40 (03) (2004) 251–256, <https://doi.org/10.3321/j.issn:0412-1961.2004.03.006>.
- [21] X. Liu, C.G. Meng, C.H. Liu, Molecular dynamics study on superheating of Pd at high heating rates [J], *Phase Transitions: Multinational J.* 79 (4–5) (2006) 249–259, <https://doi.org/10.1080/0141159600689021>.
- [22] X. Liu, C.G. Meng, C.H. Liu, Melting and superheating of Ag at high heating rate [J], *Acta Phys. Chim. Sin.* 20 (03) (2004) 280–284, <https://doi.org/10.3866/PKU.WHXB20040313>.
- [23] Z.W. Cui, F. Gao, Z.H. Cui, et al., Developing a second nearest-neighbor modified embedded atom method interatomic potential for lithium [J], *Model. Simul. Mater. Sci. Eng.* 20 (01) (2012) 1–12, <https://doi.org/10.1088/0965-0393/20/1/015014>.
- [24] Q.S. Mei, K. Lu, Melting and superheating of crystalline solids: from bulk to nanocrystals [J], *Prog. Mater Sci.* 52 (8) (2007) 1175–1262, <https://doi.org/10.1016/j.jpmatsci.2007.01.001>.

- [25] X.M. Bai, M. Li, Nature and extent of melting in superheated solids: Liquid-solid coexistence model [J], Phys. Rev. B 72 (05) (2005), 052108, <https://doi.org/10.1103/PhysRevB.72.052108>.
- [26] K. Lu, Y. Li, Homogeneous nucleation catastrophe as a kinetic stability limit for superheated crystal [J], Phys. Rev. Lett. 80 (20) (1998) 4474–4477, <https://doi.org/10.1103/PhysRevLett.80.4474>.
- [27] A. Nichol, G.J. Ackland, Property trends in simple metals: an empirical potential approach [J], Phys. Rev. B 93 (18) (2016), 184101, <https://doi.org/10.1103/PhysRevB.93.184101>.
- [28] S. Nosé, A unified formulation of the constant temperature molecular dynamics methods [J], J. Chem. Phys. 81 (1) (1984) 511–519, <https://doi.org/10.1063/1.447334>.
- [29] J.K. Fink, L. Leibowitz, Thermodynamic and transport properties of sodium liquid and vapor [M], United States: Technical Reports (1995), <https://doi.org/10.2172/94649>.
- [30] O.J. Foust, H.J. Bommelburg, C. Smith, et al. Sodium-NaK Engineering handbook Volume I: Sodium Chemistry and Physical Properties [M], Gordon and Breach, Science Publishers, Inc. 1973. <https://www.osti.gov/servlets/purl/4631555>.
- [31] Y.J. Hou, J.Y. Liu, L. Li, et al., Molecular dynamics simulation for melting process of single-crystal Aluminum [J], J. Shanxi Univ. (natural Science Edition) 3 (416–420) (2013), [https://doi.org/10.13451/j.cnki.shanxi.univ\(nat.sci.\).2013.03.030](https://doi.org/10.13451/j.cnki.shanxi.univ(nat.sci.).2013.03.030).
- [32] Y. Waseda, The Structure of Non-Crystalline Materials: Liquids and Amorphous Solids [M], McGraw-Hill International Book Co, New York, 1980. ISBN 007068426X :9780070684263.
- [33] T. Zhang, X.R. Zhang, L. Guan, et al., The simulation of metal Cu in the melting and solidification process [J], Acta Metall. Sin. 3 (2004) 251–256. <https://www.ams.org.cn/CN/Y2004/V40/I3/251>.
- [34] A.K. Metya, A. Hens, J.K. Singh, Molecular dynamics study of vapor-liquid equilibria and transport properties of sodium and lithium based on EAM potentials [J], Fluid Phase Equilib. 313 (2012) 16–24, <https://doi.org/10.1016/j.fluid.2011.08.026>.
- [35] M.W. Ozelton, R.A. Swalin, Self-diffusion in liquid sodium at constant volume and constant pressure [J], Phil. Mag. 18 (153) (2006) 441–451, <https://doi.org/10.1080/14786436808227451>.
- [36] R.E. Meyer, N.H. Nachtrieb, Self-diffusion of liquid sodium [J], J. Chem. Phys. 23 (1955) 1851–1854. <https://doi.org/10.1063/1.1740591>.
- [37] D.K. Belashchenko, Computer simulation of liquid metals [J], Phys. Usp. 56 (12) (2013) 1176–1216, <https://doi.org/10.3367/UFNr.0183.201312b.1281>.
- [38] A.K. Metya, A. Hens, J.K. Singh, Molecular dynamics study of vapor-liquid equilibria and transport properties of sodium and lithium based on EAM potentials [J], Fluid Phase Equilib. 313 (2012) 16–24, <https://doi.org/10.1016/j.fluid.2011.08.026>.
- [39] J.H. Adams, M. Ammons, H.S. Avery, et al. ASM Handbook (Volume 2), Properties and selection: Nonferrous alloys and pure metals [M]. Metals Handbook 2(10) (1990). ISBN 0-87170-378-5 (v. 2).